

# Impact of Iterative Reconstruction Algorithms on Image Quality and Radiation Dose in Computed Tomography Scan of Patients with Malignant Pancreatic Lesions

## Abstract

**Background:** The objective of this study was to investigate the influence of iterative reconstruction (IR) algorithm on radiation dose and image quality of computed tomography (CT) scans of patients with malignant pancreatic lesions by designing a new protocol. **Methods:** The pancreas CT was performed on 40 patients (23 males and 17 females) with a 160-slice CT scan machine. The pancreatic parenchymal phase was performed in two stages: one with a usual dose of radiation and the other one after using a reduced dose of radiation. The images obtained with usual dose were reconstructed with Filtered Back Projection (FBP) method (Protocol A); and the images obtained with the reduced dose were reconstructed with both FBP (Protocol B) and IR method (Protocol C). The quality of images and radiation dose were compared among the three protocols. **Results:** Image noise was significantly lower with Protocol C (10.80) than with Protocol A (14.98) and Protocol B (20.60) ( $P < 0.001$ ). Signal-to-noise ratio and contrast-to-noise ratio were significantly higher with Protocol C than with Protocol A and Protocol B ( $P < 0.001$ ). Protocol A and Protocol C were not significantly different in terms of image quality scores. Effective dose was reduced by approximately 48% in Protocol C compared with Protocol A ( $1.20 \pm 0.53$  mSv vs.  $2.33 \pm 0.86$  mSv,  $P < 0.001$ ). **Conclusion:** Results of this study showed that applying the IR method compared to the FBP method can improve objective image quality, maintain subjective image quality, and reduce the radiation dose of the patients undergo pancreas CT.

**Keywords:** *Computed tomography, image quality, iterative reconstruction, pancreas cancer, radiation dose*

Submitted: 17-Dec-2020

Revised: 06-Jan-2021

Accepted: 03-Feb-2021

Published: 28-Dec-2021

## Introduction

Pancreatic cancer is one of the most fatal cancers of the gastrointestinal system with an incidence rate of 2.5% among all cancers in both sexes and ranks seventh with a mortality rate of 4.5% and 432,242 people per year worldwide.<sup>[1]</sup> It is the third leading cause of cancer deaths in both sexes in 2020 in the United States according to the American Cancer Society.<sup>[2,3]</sup> Pancreatic cancer is difficult to diagnose in the early stages and does not cause symptoms, so it is diagnosed when the disease has advanced.<sup>[4]</sup> Evaluation of primary tumor and surrounding organs such as the celiac artery, the superior mesenteric artery, the superior mesenteric vein, the portal vein, and the hepatic artery are crucial in determining resectability.<sup>[5]</sup>

This is an open access journal, and articles are distributed under the terms of the Creative Commons Attribution-NonCommercial-ShareAlike 4.0 License, which allows others to remix, tweak, and build upon the work non-commercially, as long as appropriate credit is given and the new creations are licensed under the identical terms.

For reprints contact: [WKHLRPMedknow\\_reprints@wolterskluwer.com](mailto:WKHLRPMedknow_reprints@wolterskluwer.com)

Computed tomography (CT) is one of the top modalities for the diagnosis of malignant lesions of the pancreas. The sensitivity of CT in this case is about 90%.<sup>[6]</sup> Although the advantages of justified and accurate CT scans are far greater than their potential risks, there is often a great deal of concern about the dangers of ionizing radiation used in CT scans. Exposure to these beams increases the likelihood of cancer in the person being exposed.<sup>[7-9]</sup> Most patients with pancreatic cancer undergo CT imaging, some for initial diagnosis and some at regular intervals to evaluate response to treatment. Hence, radiation dose control along with maintaining image quality is important.

In designing new generations of CT scans, special consideration has been paid to the subject of radiation dose and new strategies of dose reduction have come to the forefront

**How to cite this article:** Asemanrafat M, Chaparian A, Lotfi M, Rasekhi A. Impact of iterative reconstruction algorithms on image quality and radiation dose in computed tomography scan of patients with malignant pancreatic lesions. *J Med Sign Sens* 2022;12:69-75.

Mohamadhosein Asemanrafat<sup>1</sup>,  
Ali Chaparian<sup>1</sup>,  
Mehrza Lotfi<sup>2</sup>,  
Alireza Rasekhi<sup>2</sup>

<sup>1</sup>Department of Medical Physics, Isfahan University of Medical Sciences, Isfahan, <sup>2</sup>Department of Radiology, Shiraz University of Medical Sciences, Shiraz, Iran

## Address for correspondence:

Prof. Ali Chaparian,  
Department of Medical Physics,  
Isfahan University of Medical  
Sciences, Isfahan, Iran.  
E-mail: [ali\\_chaparian@yahoo.com](mailto:ali_chaparian@yahoo.com)

## Access this article online

Website: [www.jmssjournal.net](http://www.jmssjournal.net)

DOI: 10.4103/jmss.JMSS\_81\_20

## Quick Response Code:



of design.<sup>[10]</sup> The usual method of image reconstruction in CT scan is the Filtered Back Projection (FBP). Due to the high speed of image creation in the FBP technique, most specialists and radiologists prefer to use this kind of images for interpreting the CT data. However, the radiation dose imposed by the FBP method is high.<sup>[11,12]</sup> Recently, new image reconstruction algorithms have been introduced, and the manufacturers believe that these techniques can considerably reduce patients' dose and preserve image quality. One of these new methods is Iterative Reconstruction (IR) algorithms, which is based on image noise reduction due to multiple cycles of repetition.<sup>[13-15]</sup> However, these new image reconstruction methods are not yet accepted mentally and visually.<sup>[16]</sup> Adaptive iterative dose reduction-three dimensional (AIDR 3D) is an IR technique that allows the operator to alter the noise level of image by a factor called "AIDR 3D level."

To date, only a few studies have been conducted on the impact of new methods of image reconstruction on radiation dose and image quality of the pancreatic cancer CT examination.<sup>[17-20]</sup> Xie *et al.*<sup>[17]</sup> evaluated the effects of an IR algorithm (iDose) on the images of CT perfusion of the pancreas obtained with a 256-slice CT scanner. In another study conducted by Yamamura *et al.*,<sup>[18]</sup> patients with malignant pancreatic lesions were examined with a 64-slice CT scanner. They evaluated the impact of a low-tube-voltage technique and hybrid IR (iDose) on image quality at dynamic CT of the pancreas. The purpose of our study was to investigate the effects of an IR algorithm (AIDR 3D; Toshiba) on radiation dose and image quality of CT scans of the patients with malignant pancreatic lesions performed with a 160-slice CT scan machine by designing a new protocol.

## Materials and Methods

### Ethics

This study was a prospective clinical trial conducted which had been approved by the Research Ethics Committee of Isfahan University of Medical Sciences with ID number IR.MUI.MED.REC.1398.316. This study was also registered at the Iranian Registry of Clinical Trials site with ID number: IRCT20190930044930N1. Written informed consent was acquired from all participants.

### Patients

The study population consisted of 40 patients (23 males and 17 females; mean age:  $62.55 \pm 7.16$  [48–73]) who had previously been diagnosed with pancreatic cancer. They were referred to the department of CT, Abu-Ali Sina Hospital, Shiraz, Iran (Subspecialty Organ Transplants Center) between January 2019 and January 2020. Abdomen and pelvic CT scans with the pancreatic protocol were performed to assess the response to treatment or the feasibility of surgical resection of the pancreatic lesion.

Exclusion criteria for the examination were any allergy to the contrast agent, renal failure with glomerular filtration rate  $<45$ , body mass index (BMI)  $>30$ , inappropriate physical conditions such as inability to breath imprisonment and inability to control voluntary body movements. The mean weight, height, and BMI of patients were  $58.40 \pm 8.25$  (44–80) kg,  $166.12 \pm 5.50$  cm (150–180) cm, and  $21.08 \pm 2.03$  (17.19–26.37) kg/m<sup>2</sup>, respectively.

### Computed tomography protocols

All scans were performed with a 160-slice CT scan machine (Toshiba, Aquilion Prime SP-Canon Medical Systems-Japan). The patients were asked to drink 1000 mL of mineral water regularly 1 h before the examination to fill the stomach, duodenum, and intestines, for a better separation of the pancreas, liver, spleen, and lymph nodes from adjacent organs. Up to 15 min before CT, the patients were free to empty their bladder. Ten minutes before the test, an 18 or 20-G intravenous catheter was placed in an antecubital vein. Patients were trained to hold their breath during the imaging. All phases of the pancreas CT were performed at the end of exhalation.

In the first step, the unenhanced scan was taken from the abdominal area in the craniocaudal direction from the upper level of the diaphragm to the iliac crests. This scan was performed to achieve a baseline image of abdominal organs and the possible pancreatic calcifications.

Then, for the contrast-enhanced CT examination, at first, monitoring was performed with a 2-mm-thick slice in the diaphragm area by ScanView software (an automatic bolus-tracking program) and the thoracic-abdominal aorta was imaged and the reference region of interest (ROI) was placed on it. The contrast agent was then injected with a double-headed power injector (Nemoto-Dual Shot, Alpha 7 Kyorindo, Japan). The contrast agent used in all patients was nonionic (Omnipaque 350 mg iodine/ml; GE, Ireland). The volume of contrast material was determined based on the patient's weight, 500 mg iodine/kg and delivered at a flow rate of 4 mL/s, followed by 30 mL of saline flush serving as a bolus chaser. Eight seconds after injection, the images were dynamically taken from the monitoring site (abdominal-thoracic aorta) with a 1 s interval using the Sure Start software. After the entry of the contrast material into the target area and crossing the trigger threshold level of 180 Hounsfield units (HU), imaging of the contrast-enhanced phases was performed as follows:

- a. Arterial phase was performed 10 s after triggering. This phase was taken at a usual dose from the abdominal area (above the diaphragm to the beginning of the iliac blade) for evaluation of pancreatic endocrine lesions, abdominal arteries, and possible involvements by the pancreatic lesions
- b. Pancreatic parenchymal phase was performed 15 s after the end of the arterial phase, only from the pancreas in two stages; one by using a usual dose of radiation

and one immediately after using a reduced dose of radiation. The time interval between these two stages was set to the minimum time (3 s). In the parenchymal phase, the contrast between normal pancreatic tissue and adenocarcinoma lesions, which are mostly hypodense, reaches its maximum value. To stabilize the contrast material density and similarity of the slices in both parenchymal phase stages, the usual dose stage was performed in the direction of head to feet, and then, the reduced dose stage performed from feet to head. Furthermore, for the similar respiratory situation and co-registration of images between two stages, respiratory confinement was ordered at the beginning of the usual dose stage and respiratory release was ordered at the end of the reduced dose stage, so both stages were performed in one breath-hold episode

- c. Portal venous phase was performed with manually delay of 70 s after starting contrast injection by using a usual dose from the abdomen and pelvis (above the diaphragm to the bottom of the symphysis pubis). In this phase, the liver and spleen are seen with the highest possible density and uniformity. This phase was used to evaluate metastatic lesions of the liver and spleen or peritoneal lesions
- d. After evaluating the images of the previous phases, 7 min after injection of contrast material, a delayed phase was performed from areas with primary or metastatic lesions.

For all phases, a tube voltage of 120 kVp and automated tube current modulation (sure exposure 3D) were used. Noise Index (NI) is a tool in the scanner that controls the amount of noise in the image. It also has a direct influence on radiation dose. NI is directly proportional to image noise and inversely proportional to radiation dose. NI varies among vendors and models. In this study, we first evaluated a lot of routine standard-dose studies and most of them had NI of 8. Then, according to literature<sup>[21]</sup> and based on our system, we set NI of 12 for the low-dose phase to decrease the radiation dose to 50%. For changing radiation dose between usual dose and reduced dose stages, a NI of 8 was used for the usual dose stage and a NI of 12 for the reduced dose stage. Since radiation dose change was merely applied to the parenchymal phase, only images of this phase were chosen for subjective and objective analysis. Table 1 summarizes CT scan parameters for the two parenchymal phase stages.

### Computed tomography image reconstruction

The thickness of all reconstructed slices and the distance between them were 3 mm. The images obtained with usual dose were reconstructed with the FBP method (Protocol A). The images of the parenchymal phase obtained with the reduced dose were reconstructed with both FBP (Protocol B) and IR (AIDR 3D) (Protocol C) methods. Therefore, for each patient, three image sets were

**Table 1: Computed tomography scan parameters for the two parenchymal phase stages**

Parameters	Usual dose protocol	Reduced dose protocol
Tube voltage (kVp)	120	120
Tube current range (mA)	80-500	80-500
Rotation time (s)	0.5	0.5
Noise index	8	12
Field of view (mm)	300-400	300-400
Helical pitch (standard)	0.813	0.813
Detector configuration	0.5×80	0.5×80
Beam collimation (mm)	40	40
Slice thickness (mm)	3	3
Slice interval (mm)	3	3
Reconstruction algorithm	FBP	FBP and AIDR 3D

FBP – Filtered Back Projection; AIDR 3D – Adaptive iterative dose reduction three-dimensional

prepared. AIDR 3D has four levels as follows: enhanced, strong, standard, and mild. The higher the AIDR 3D level, the greater the noise reduction. In this study, standard level of AIDR 3D was used to achieve the optimal trade-off between noise reduction and edge depiction.

### Radiation dose

To change the radiation dose between two stages of the parenchymal phase, the NI was applied. NI controls the radiation dose of a protocol using a predefined level of the image noise. In this study, NIs of 8 and 12 were used for the usual dose stage and reduced dose stage, respectively. For all patients, the volume CT dose index ( $CTDI_{vol}$ ) and dose-length product (DLP) were obtained at the end of each phase. The accuracy of the displayed CTDI and DLP values had been validated by measuring doses with a pencil probe solid-state dosimeter in a polymethyl-methacrylate phantom according to the specific guidelines. The effective dose was also obtained by multiplying the DLP by a constant factor of 0.015 mSv/mGy/cm.<sup>[22]</sup>

### Quantitative image analysis

The images of the parenchymal phase were transferred to a viewer software (RadiAnt DICOM Viewer, Medixant, Poznan, Poland). Quantitative evaluation was accomplished by placing a manually defined ROI on the pancreatic parenchyma, portal vein, abdominal aorta, liver, and paraspinal muscles [Figure 1]. The number of pixels of ROI was 150-300. The mean CT attenuation values (in HUs) of ROIs were used as the tissues attenuation values. The ROIs were carefully drawn so that not so small to be influenced by pixel variation and not so large to include areas with high spatial density variability such as small vessels and the calcifications. Pancreatic attenuation was measured as the mean HUs of three areas on the head, body, and tail. Average of these three areas was determined as mean HUs of the pancreas. Liver attenuation was also measured as the mean HUs of three areas on the left lobe as well as on the

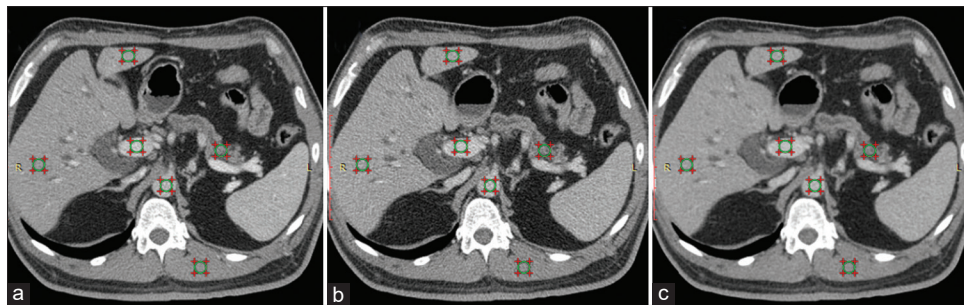


**Figure 1:** Axial contrast-enhanced computed tomography images of a 62-year-old male in the pancreatic parenchymal phase showing region of interests on the pancreas, portal vein, abdominal aorta, and liver. (a) Usual dose with Filtered Back Projection. (b) Reduced dose with Filtered Back Projection. (c) Reduced dose with adaptive iterative dose reduction three dimensional

anterior and posterior segment of the right lobe. Average of these three areas was determined as mean HUs of the Liver.

The signal-to-noise ratio (SNR) were determined by dividing the mean CT numbers of each tissue by the noise. Image noise for all protocols was defined as the standard deviation of pixels in the uniform area of the paraspinal muscle tissue.

$$\text{SNR} = \text{ROI}_{\text{tiss}} / \text{standard deviation (SD)}_m \quad (1)$$

The contrast-to-noise ratio (CNR) was determined by dividing the contrast and noise. The contrast was the absolute value of the difference between the attenuation value of each tissue (portal vein, the abdominal aorta, and liver) and the paraspinal muscle.

$$\text{CNR} = |\text{ROI}_{\text{tiss}} - \text{ROI}_m| / \text{SD}_m \quad (2)$$

However, for the pancreas, the contrast was the absolute value of the difference between the attenuation value of the normal pancreatic parenchyma and the pancreatic tumor, and the noise was also determined as the standard deviation of pixels in the normal pancreatic parenchyma.

$$\text{CNR}_{\text{Pan}} = |\text{ROI}_{\text{Pan}} - \text{ROI}_{\text{Tum}}| / \text{SD}_{\text{Pan}} \quad (3)$$

### Qualitative image analysis

Two radiologists with 18 and 23 years of experience in interpretation of the abdominal and pelvic CT evaluated all images independently. None of two radiologists was involved in the designing and implementation of the CT protocols. The images were displayed to the two radiologists randomly. To prevent the detection of image information and the type of image reconstruction, all image data were erased from the images and all image sets were encoded. The window level and width were 40 and 400, respectively, but radiologists were allowed to change these values. Conditions for viewing the images including room light and monitor quality were identical and were in the order of most reading rooms. They scored the images based on indices such as the density of the pancreas and adjacent organs, tumor depiction, noise, artifacts as well as spatial and contrast resolutions [Figure 2]. The radiologists used a 5-point Likert scale for qualitative image evaluation:

score of 5 – Excellent: the density of pancreatic tissue and adjacent organs such as liver, spleen, kidney, and adrenal glands were excellent and pancreatic duct, calcification, and possible necrosis were easily seen. The location of the lesion and its dimensions were easily identifiable, and the adjacent vessels such as superior mesenteric artery, celiac artery, the portal vein, the superior mesenteric vein, and its involvements with the lesion were easily seen. The noise and artifacts in the image were minimal and the spatial resolution and contrast were excellent. Score of 4 – Good: the density of pancreatic tissue and adjacent organs was good. Pancreatic ducts, calcification, and possible necrosis were seen. The location of the lesion and its dimensions were detectable and the adjacent vessels and their involvement with the lesion were seen. Noise and artifacts were usual and did not harm the diagnosis. Spatial and contrast resolution were suitable. Score of 3 – Acceptable: the density of pancreatic tissue and adjacent organs was acceptable. Pancreatic lesion and its dimensions were detectable and minimally compromised by image noise. The pancreatic duct, calcification, possible necrosis, adjacent arteries, and edges were slightly affected by noise and artifacts, but the image is still detectable. Spatial and contrast resolution had somewhat distorted. Score of 2 – Poor: the density of pancreatic tissue and adjacent organs as well as the location and dimensions of the lesion were significantly affected by noise and artifacts. The pancreatic duct and calcification and possible necrosis were hardly seen because of noise and artifacts. The vascular edges were not clear. Spatial and contrast resolution were completely reduced. Score of 1 – Unacceptable: the image was indistinguishable and unacceptable because of high noise and artifacts in the image, as well as distortion of spatial and contrast resolution.

If the images scored 3–5, they were considered distinguishable, and if they scored 1 and 2, they were considered indistinguishable.

### Statistical analysis

Statistical analysis was performed with SPSS Statistics version 19 (SPSS Inc., Chicago, IL, USA). Different parameters (CT number, image noise, SNR, CNR,

image quality score,  $CTDI_{vol}$ , DLP, and effective dose) were expressed as the means  $\pm$  SDs. For evaluation of differences between the images obtained with usual radiation dose and reduced radiation dose parenchymal phase stages, the paired *t*-test was used. A  $P < 0.05$  was considered statistically significant. The degree of agreement between the two radiologists at qualitative image analysis was measured using the Kappa test. The kappa value can be interpreted as 0–0.20, poor; 0.21–0.40, fair; 0.41–0.60, moderate; 0.61–0.80, good; and 0.81–1.00, excellent agreement.

## Results

### Quantitative image quality analysis

Table 2 summarizes SNR and CNR in the pancreatic parenchyma, portal vein, abdominal aorta, and liver. The noise was also calculated in the pancreatic parenchyma and paraspinal muscle.

Mean image noise was significantly lower with Protocol C (10.80) than with Protocol A (14.98) and Protocol

B (20.60) ( $P < 0.001$ ). The mean SNRs and CNRs of the pancreatic parenchyma, portal vein, abdominal aorta, and liver were significantly higher with Protocol C than with Protocol A and Protocol B.

### Qualitative image quality analysis

The results of the qualitative image analysis evaluated by the two radiologists are shown in Table 3. The mean image quality scores in Protocol B were significantly lower than the other protocols ( $P < 0.01$ ); there was no significant difference between Protocol A and Protocol C. Interobserver agreements on image scores were good ( $\kappa = 0.78$ ).

### Radiation dose

During the CT scan of the pancreas, the average  $CTDI_{vol}$  for Protocols B and C ( $4.23 \pm 1.10$  mGy) was significantly less than that for Protocol A ( $8.17 \pm 1.84$  mGy) ( $P < 0.001$ ). The average DLP for Protocols B and C ( $80.12 \pm 35.11$  mGy.cm) was significantly lower than that for Protocol A ( $155.34 \pm 57.29$  mGy.cm) ( $P < 0.001$ ). Similarly, the

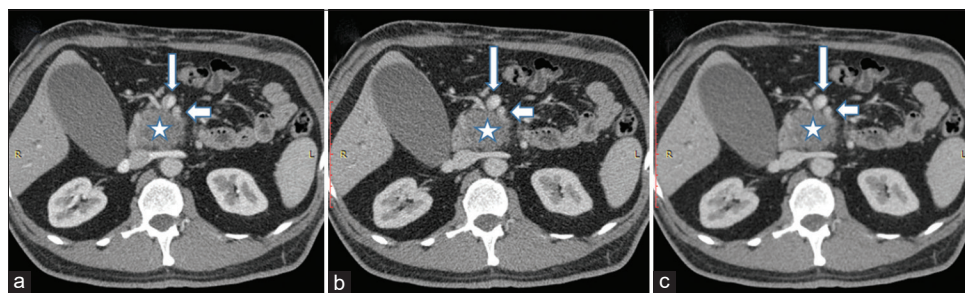


Figure 2: Axial contrast-enhanced computed tomography images of a 62-year-old male in the pancreatic parenchymal phase showing adenocarcinoma in the head of pancreas (star) and the encasement of superior mesenteric vein (long arrow) and celiac trunk (short arrow) by the lesion. (a) Usual dose with Filtered Back Projection. (b) Reduced dose with Filtered Back Projection. (c) Reduced dose with adaptive iterative dose reduction three dimensional

Table 2: Quantitative assessment of image quality of the pancreas computed tomography for Protocols A, B, and C

Parameters	Protocols*			P		
	A	B	C	A versus B	A versus C	B versus C
Pancreatic parenchyma						
Noise	19.58 $\pm$ 4.34	25.13 $\pm$ 5.12	13.40 $\pm$ 3.17	<0.001	<0.001	<0.001
SNR	5.4 $\pm$ 2.13	3.97 $\pm$ 1.49	7.5 $\pm$ 3.12	<0.001	<0.001	<0.001
CNR	3.55 $\pm$ 2	2.46 $\pm$ 1.37	4.68 $\pm$ 2.79	0.005	0.04	<0.001
Portal vein						
SNR	10.79 $\pm$ 2.65	7.79 $\pm$ 1.94	14.49 $\pm$ 2.89	<0.001	<0.001	<0.001
CNR	6.52 $\pm$ 1.78	4.65 $\pm$ 1.36	8.51 $\pm$ 2.08	<0.001	<0.001	<0.001
Abdominal aorta						
SNR	10.44 $\pm$ 3.14	6.98 $\pm$ 1.65	12.77 $\pm$ 2.38	<0.001	<0.001	<0.001
CNR	6.16 $\pm$ 2.73	3.84 $\pm$ 1.11	6.87 $\pm$ 1.67	<0.001	0.045	<0.001
Liver						
SNR	5.28 $\pm$ 1.56	4.46 $\pm$ 1.23	8.36 $\pm$ 2.09	0.01	<0.001	<0.001
CNR	1.17 $\pm$ 0.64	1.40 $\pm$ 0.57	2.58 $\pm$ 1.01	0.045	<0.001	<0.001
Paraspinal muscle						
Noise	14.98 $\pm$ 3.23	20.60 $\pm$ 4.19	10.80 $\pm$ 1.95	<0.001	<0.001	<0.001

\*Protocol A: The images which obtained at usual dose and reconstructed with the FBP, Protocol B: The images which obtained at reduced dose and reconstructed with FBP, Protocol C: The images which obtained at reduced dose and reconstructed with AIDR 3D. SNR – Signal-to-noise ratio; CNR – Contrast-to-noise ratio; FBP – Filtered back projection; AIDR 3D – Adaptive iterative dose reduction three dimensional

average estimated effective dose for Protocols B and C ( $1.20 \pm 0.53$  mSv) was significantly lower than that for Protocol A ( $2.33 \pm 0.86$  mSv) ( $P < 0.001$ ) [Table 4]. Therefore, a radiation dose reduction of about 48% was attained with the low dose technique.

### Discussion

The pancreas CT is a useful method for diagnoses of the malignant pancreatic lesions, however, risks related to radiation exposure from CT are a continuous concern. At present, CT vendors have developed various IR techniques and claim that these techniques can reduce the patient's dose and improve image quality. The results of the present study showed that the implementation of the IR (AIDR 3D) technique could reduce radiation dose and quantitatively improve image quality compared with the conventional FBP technique.

Our quantitative evaluation demonstrated that image reconstruction of the reduced radiation dose CT data of the parenchymal phase with IR technique (AIDR 3D) (Protocol C) yielded significant reduced image noise and improvements in CNR and SNR compared with the FBP technique (Protocols A and B). The qualitative evaluation showed that the overall image quality for Protocol B ( $3.69 \pm 0.64$ ) was significantly lower than that for Protocols A and C ( $4.36 \pm 0.50$  and  $4.18 \pm 0.54$ ) ( $P < 0.001$ ). However, there were no significant differences in the overall image quality among Protocols A and C ( $P = 0.13$ ). IR images are somehow different from routine FBP images and there may be a slight resistance from clinicians to accept these images in daily practice. However, regarding the dose savings both to the patient and equipment, it is necessary to consider image quality along with dose reduction. Similar to the current study, Xie *et al.*<sup>[17]</sup> and Yamamura *et al.*<sup>[18]</sup> have also used IR techniques in the pancreas CT and quantitatively and qualitatively evaluated images from different methods of image reconstruction. They have also shown the reduction of patients' dose while maintaining or even enhancing

image quality. However, the limitation of Xie *et al.*<sup>[17]</sup> study was that images from different image reconstructions were obtained and compared in different patients. Furthermore, there was a similar limitation in Yamamura *et al.*<sup>[18]</sup> study so that the pancreatic tissue and the lesions and vessels might undergo changes during chemotherapy that made it difficult to compare images before and after chemotherapy. To overcome these limitations, we designed a pancreas CT scan technique that had two closely timed stages through the pancreas during the parenchymal phase. The first stage was performed with usual radiation dose and images were reconstructed with FBP. The second stage was performed with the reduced radiation dose and images were reconstructed with IR and FBP. This technique was also performed by Shuman *et al.*<sup>[21]</sup> for the liver CT scan.

In the current study, with the reduced dose protocol, the radiation dose was reduced by approximately 48% compared with the conventional standard-dose protocol. The studies of Xie *et al.*<sup>[17]</sup> and Yamamura *et al.*<sup>[18]</sup> have also reported that with the IR technique, a significant dose reduction of 54% and 44%, respectively, could be achieved. They recognized that IR technique obviously decreased noise of images and increased subjective and objective image quality.

There were some limitations in the present study. First, the image reconstruction algorithm of AIDR 3D is unique to Toshiba, and our results may not be applicable to other IR algorithms from other manufactures. Second, effective dose was calculated by multiplying the DLP by a constant factor while this method of calculation is not very accurate. Third, it was hard to blind the radiologists to the reconstruction methods because the appearance of the images of each method was somewhat different and unique. However, the type of image reconstruction and all image data were erased from the images and presented in a randomized order. Two radiologists who participated in our study had somehow different attitudes toward image components such as spatial and contrast resolution but both of them scored a good number to images obtained with low-dose IR method.

**Table 3: Qualitative assessment of image quality of the pancreas computed tomography for Protocols A, B, and C from the two radiologists**

Protocol	Radiologist 1			Radiologist 2			Average scores of two radiologists		
	A	B	C	A	B	C	A	B	C
Image quality score	4.35±0.48	3.83±0.75	4.15±0.58	4.38±0.54	3.55±0.50	4.20±0.52	4.36±0.50	3.69±0.64	4.18±0.54
	<b>A versus B</b>	<b>B versus C</b>	<b>A versus C</b>	<b>A versus B</b>	<b>B versus C</b>	<b>A versus C</b>	<b>A versus B</b>	<b>B versus C</b>	<b>A versus C</b>
P	<0.001	0.03	<0.09	<0.001	<0.001	0.09	<0.001	<0.001	0.13

**Table 4: Radiation dose of the pancreas computed tomography for Protocols A, B, and C**

	Protocol A (usual dose with FBP)	Protocol B or C (reduced dose)	Dose reduction (%)
CTDI <sub>vol</sub> (mGy)	8.17±1.84 (5.20-13.40)	4.23±1.10 (3.00-9.30)	48.07
DLP (mGy.cm)	155.34±57.29 (72.80-374.00)	80.12±35.11 (42.00-259.00)	48.31
Effective dose (mSv)	2.33±0.86 (1.09-5.61)	1.20±0.53 (0.63-3.89)	48.42

FBP – Filtered Back Projection; CT – Computed tomography; CTDI<sub>vol</sub> – CT dose index; DLP – Dose-length product

## Conclusion

The results of the current study showed that perspective of IR methods is promising. It demonstrated how application of IR method (AIDR 3D) compared to the conventional reconstruction method (FBP) can improve objective image quality, maintain subjective image quality, and reduce the radiation dose of the patients undergoing the pancreas CT.

## Acknowledgment

This study was sponsored by the Isfahan University of Medical Sciences with the approved project number of 398354.

## Financial support and sponsorship

This study was financially supported by Isfahan University of Medical Sciences.

## Conflicts of interest

There are no conflicts of interest.

## References

1. Bray F, Ferlay J, Soerjomataram I, Siegel RL, Torre LA, Jemal A. Global cancer statistics 2018: GLOBOCAN estimates of incidence and mortality worldwide for 36 cancers in 185 countries. *CA Cancer J Clin* 2018;68:394-424.
2. Siegel RL, Miller KD, Jemal A. Cancer statistics, 2019. *CA Cancer J Clin* 2019;69:7-34.
3. American Cancer Society. Cancer Statistics Center. Available from: <http://cancerstatisticscenter.cancer.org>. [Last accessed on 2020 Feb 10].
4. Tempero MA, Malafa MP, Al-Hawary M, Asbun H, Bain A, Behrman SW, *et al.* Pancreatic adenocarcinoma, version 2.2017, NCCN clinical practice guidelines in oncology. *J Natl Compr Canc Netw* 2017;15:1028-61.
5. Vincent A, Herman J, Schulick R, Hruban RH, Goggins M. Pancreatic cancer. *Lancet* 2011;378:607-20.
6. Brennan DD, Zamboni GA, Raptopoulos VD, Kruskal JB. Comprehensive preoperative assessment of pancreatic adenocarcinoma with 64-section volumetric CT. *Radiographics* 2007;27:1653-66.
7. Brenner DJ, Hall EJ. Computed tomography – An increasing source of radiation exposure. *N Engl J Med* 2007;357:2277-84.
8. Chaparian A, Zarchi HK. Assessment of radiation-induced cancer risk to patients undergoing computed tomography angiography scans. *Int J Radiat Res* 2018;16:107-15.
9. Mahmoodi M, Chaparian A. Organ doses, effective dose, and cancer risk from coronary CT angiography examinations. *AJR Am J Roentgenol* 2020;214:1131-6.
10. McCollough CH, Bruesewitz MR, Kofler JM Jr. CT dose reduction and dose management tools: Overview of available options. *Radiographics* 2006;26:503-12.
11. Jiang H. *Computed Tomography: Principles, Design, Artifacts, and Recent Advances*. Bellingham, Washington USA (Published by SPIE and John Wiley & Sons, Inc.): SPIE; 2009.
12. Prakash P, Kalra MK, Kambadakone AK, Pien H, Hsieh J, Blake MA, *et al.* Reducing abdominal CT radiation dose with adaptive statistical iterative reconstruction technique. *Invest Radiol* 2010;45:202-10.
13. Beister M, Kolditz D, Kalender WA. Iterative reconstruction methods in X-ray CT. *Phys Med* 2012;28:94-108.
14. Leipsic J, Nguyen G, Brown J, Sin D, Mayo JR. A prospective evaluation of dose reduction and image quality in chest CT using adaptive statistical iterative reconstruction. *AJR Am J Roentgenol* 2010;195:1095-9.
15. Woitschläger M, Henriksson L, Bartholomae W, Gasslander T, Björnsson B, Sandström P. Iterative reconstruction algorithm improves the image quality without affecting quantitative measurements of computed tomography perfusion in the upper abdomen. *Eur J Radiol Open* 2020;7:100243.
16. Mileto A, Guimaraes LS, McCollough CH, Fletcher JG, Yu L. State of the art in abdominal CT: The limits of iterative reconstruction algorithms. *Radiology* 2019;293:491-503.
17. Xie Q, Wu J, Tang Y, Dou Y, Hao S, Xu F, *et al.* Whole-organ CT perfusion of the pancreas: Impact of iterative reconstruction on image quality, perfusion parameters and radiation dose in 256-slice CT-preliminary findings. *PLoS One* 2013;8:e80468.
18. Yamamura S, Oda S, Utsunomiya D, Funama Y, Imuta M, Namimoto T, *et al.* Dynamic computed tomography of locally advanced pancreatic cancer: Effect of low tube voltage and a hybrid iterative reconstruction algorithm on image quality. *J Comput Assist Tomogr* 2013;37:790-6.
19. Yasaka K, Katsura M, Akahane M, Sato J, Matsuda I, Ohtomo K. Model-based iterative reconstruction and adaptive statistical iterative reconstruction: Dose-reduced CT for detecting pancreatic calcification. *Acta Radiol Open* 2016;5:2058460116628340.
20. Choi JW, Lee JM, Yoon JH, Baek JH, Han JK, Choi BI. Iterative reconstruction algorithms of computed tomography for the assessment of small pancreatic lesions: Phantom study. *J Comput Assist Tomogr* 2013;37:911-23.
21. Shuman WP, Chan KT, Busey JM, Mitsumori LM, Choi E, Koprowicz KM, *et al.* Standard and reduced radiation dose liver CT images: Adaptive statistical iterative reconstruction versus model-based iterative reconstruction-comparison of findings and image quality. *Radiology* 2014;273:793-800.
22. Deak PD, Smal Y, Kalender WA. Multisection CT protocols: Sex- and age-specific conversion factors used to determine effective dose from dose-length product. *Radiology* 2010;257:158-66.